JOC*Article*

Ring Opening of 2,5-Didehydrothiophene: Matrix Photochemistry of C_4H_2S Isomers

Yong Seol Kim, Hiroshi Inui, and Robert J. McMahon*

Department of Chemistry, University of Wisconsin, 1101 University Avenue, Madison, Wisconsin 53706

mcmahon@chem.wisc.edu

Received August 11, 2006

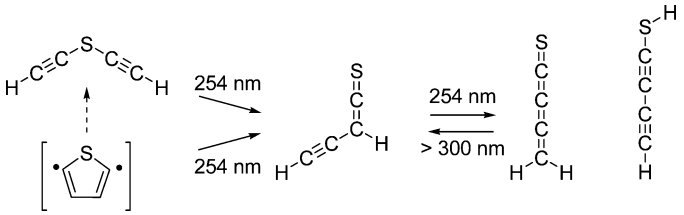

Irradiation (λ > 254 nm) of matrix-isolated 2,5-diiodothiophene (**10**) gives rise to IR bands assigned to ethynylthioketene (**6**). Diethynyl sulfide (**3**), which would form in the process of retro-Bergman cyclization of the incipient 2,5-didehydrothiophene (**4**), is not detected. Under the same irradiation conditions, matrix-isolated diethynyl sulfide (**3**) rearranges to thioketene **6** and butatrienethione (**5**), the global minimum on C_4H_2S potential energy surface. The photochemical formation of thioketene **6** from either diyl **4** or sulfide **3** may be interpreted in line with a recent computational prediction on the thermal ring opening of diyl **4**, which favors C−S bond cleavage, leading to **6**, over C−C bond cleavage, leading to **3**. Photolysis of matrix-isolated 3,4-thiophenedicarboxylic acid anhydride (**11**) enables the observation of the photoequilibration of three low-energy C_4H_2S isomers, butatrienethione (**5**), ethynylthioketene (**6**), and butadiynylthiol (**7**), via apparent [1,3]-hydrogen shifts.

Introduction

The current mechanistic investigation of C_4H_2S isomers combines matrix-isolation spectroscopy and computational studies to investigate a Bergman-type cycloaromatization reaction and relevant photochemistry in the context of hetero-aryne and cumulene chemistry. Sulfur-containing carbon cumulenes similar to those described in the current investigation have recently been studied by rotational spectroscopy[1,2] and detected in space by radioastronomy.[3−6]

Ever since Jones and Bergman postulated the intermediacy of *p*-benzyne (**2**) in the thermal isomerization reaction of *cis*-hex-3-ene-1,5-diyne (**1**),[7,8] there has been remarkable progress leading to the current detailed understanding of enediyne cycloaromatization reactions (Figure 1).[9−20] In conjunction with potential materials applications,[21−26] Bergman-type cycloaromatization reactions, including the diethynyl sulfide (**3**) system,[27−31] have recently received attention. Just as with the parent enediyne

(1) Gordon, V. D.; McCarthy, M. C.; Apponi, A. J.; Thaddeus, P. *Astrophys. J. Suppl. Ser.* **2001**, *134*, 311−317.
(2) Gordon, V. D.; McCarthy, M. C.; Apponi, A. J.; Thaddeus, P. *Astrophys. J. Suppl. Ser.* **2002**, *138*, 297−303.
(3) Saito, S.; Kawaguchi, K.; Yamamoto, S.; Ohishi, M.; Suzuki, H.; Kaifu, N. *Astrophys. J.* **1987**, *317*, L115−L119.
(4) Yamamoto, S.; Saito, S.; Kawaguchi, K.; Kaifu, N.; Suzuki, H.; Ohishi, M. *Astrophys. J.* **1987**, *317*, L119−L121.
(5) Cernicharo, J.; Guélin, M.; Hein, H.; Kahane, C. *Astron. Astrophys.* **1987**, *181*, L9−L12.
(6) Bell, M. B.; Avery, L. W.; Feldman, P. A. *Astrophys. J.* **1993**, *417*, L37−L40.
(7) Jones, R. R.; Bergman, R. G. *J. Am. Chem. Soc.* **1972**, *94*, 660−661.
(8) Bergman, R. G. *Acc. Chem. Res.* **1973**, *6*, 25−31.
(9) Hoffmann, R.; Imamura, A.; Hehre, W. J. *J. Am. Chem. Soc.* **1968**, *90*, 1499−1509.
(10) Roth, W. R.; Hopf, H.; Horn, C. *Chem. Ber.* **1994**, *127*, 1765−1779.
(11) Kraka, E.; Cremer, D. *Chem. Phys. Lett.* **1993**, *216*, 333−340.
(12) Kraka, E.; Cremer, D. *J. Am. Chem. Soc.* **1994**, *116*, 4929−4936.
(13) Wenthold, P. G.; Squires, R. R.; Lineberger, W. C. *J. Am. Chem. Soc.* **1998**, *120*, 5279−5290.
(14) Wenthold, P. G.; Squires, R. R. *J. Am. Chem. Soc.* **1994**, *116*, 6401−6412.
(15) Marquardt, R.; Balster, A.; Sander, W.; Kraka, E.; Cremer, D.; Radziszewski, J. G. *Angew. Chem., Int. Ed.* **1998**, *37*, 955−958.
(16) Cramer, C. J. *J. Am. Chem. Soc.* **1998**, *120*, 6261−6269.
(17) McMahon, R. J.; Halter, R. J.; Fimmen, R. L.; Wilson, R. J.; Peebles, S. A.; Kuczkowski, R. L.; Stanton, J. F. *J. Am. Chem. Soc.* **2000**, *122*, 939−949.
(18) Gräfenstein, J.; Hjerpe, A. M.; Kraka, E.; Cremer, D. *J. Phys. Chem. A* **2000**, *104*, 1748−1761.
(19) Crawford, T. D.; Kraka, E.; Stanton, J. F.; Cremer, D. *J. Chem. Phys.* **2001**, *114*, 10638−10650.
(20) Wenk, H. H.; Winkler, M.; Sander, W. *Angew. Chem., Int. Ed.* **2003**, *42*, 503−528.

10.1021/jo061678l CCC: $33.50
Published on Web 11/30/2006

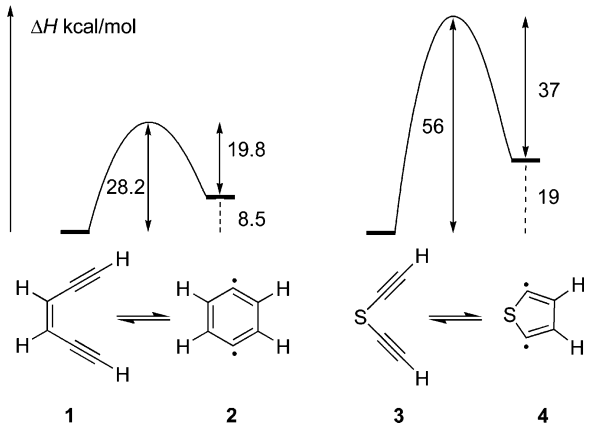

FIGURE 1. Potential energy diagrams for the cycloaromatization reactions of *cis*-hex-3-ene-1,5-diyne (**1**)[10] and diethynyl sulfide (**3**).[27]

1,[17] the equilibrium structure of sulfide **3** is symmetric (C_{2v}) and floppy, by virtue of low-frequency deformation modes.[28] In contrast to enediyne **1**, however, sulfide **3** faces a high activation barrier (ca. 60 kcal/mol) toward the formation of thiophene-2,5-diyl (**4**) (Figure 1).[27,30] Photolysis of substituted diethynyl sulfides in solution indeed affords products resulting from the cycloaromatization reaction, albeit in quite low yields.[29]

We recently noted that diethynyl sulfide (**3**) lies quite high in energy on the C_4H_2S potential energy surface (PES), hinting at the possibility for rearrangement to lower-lying isomers. Indeed, an alternative ring-opening pathway of 2,5-didehydrothiophene (**4**) exists, with an activation barrier 2-fold lower than that for the formation of sulfide **3** (Scheme 1).[30] Accordingly, one can appreciate the difficulty in trapping[29] or characterizing the incipient diradical **4** during the cycloaromatization reaction of sulfide **3** since the barrier to C−S cleavage, leading to ethynylthioketene (**6**), is significantly lower than the barrier to the initial cycloaromatization event. Photolysis of precursors to 2,3- and 3,4-didehydrothiophene also affords ring-opened products.[32] In line with our recent computational study, herein we report matrix photochemistry associated with C_4H_2S isomers **3**−**7**, which provides a better understanding of the interconversions on this potential energy surface (Scheme 1).

Results and Discussion

Compounds for Matrix-Isolation Study. Diethynyl sulfide (**3**), 2,5-diiodothiophene (**10**), and 3,4-thiophenedicarboxylic acid anhydride (**11**)[32] were used to access the C_4H_2S potential energy surface. Unlike the other two precursors, diethynyl sulfide (**3**) posed a significant challenge in preparing matrices of high purity and spectroscopic quality. In the following section, we describe a successful occasion of depositing **3** in a N_2 matrix, reserving preparation details (N_2 and Ar matrices) for the Supporting Information.

SCHEME 1[a]

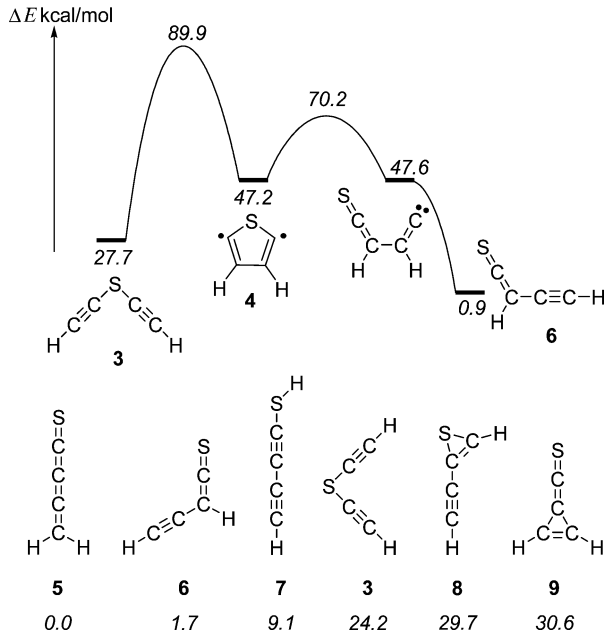

[a] Relative energy (kcal/mol) in italics. Potential energy diagram at CCSD(T)/cc-pVDZ; six low-energy isomers on C_4H_2S PES at CCSD(T)/cc-pVTZ (ZPVE corrected).[30]

TABLE 1. Computed and Experimental Mid-IR Frequencies and Intensities of Diethynyl Sulfide (3)

	CCSD(T)/cc-pVDZ[a]		in N_2[b]		in Ar[b,c]	
symmetry	frequency	*I*	frequency	area	frequency	area
a_1	3465.3	41.4	3318	15.4	3313	
b_2	3464.4	111.9	3312			
			3305			
b_2	2099.1	4.1	2064	0.3	2068	0.6
			2060		2062	
b_2	711.7	4.7	710	2.3	710	1.3
a_1	692.1	21.2	705		703	
a_1	663.7	22.6	695	3.5	683	3.2
b_2	663.6	19.1				
b_1	535.4	85.2	580	7.3	563	3.6
a_1	458.4	19.5	471	1.6	471	2.1

[a] Unscaled frequencies in cm^{-1} and computed intensities in km/mol. [b] At 10 K; total integrated area under each absorption or group of closely spaced absorptions. [c] Band assignments of **3** less satisfying, due to the interference by impurities. See Supporting Information for details.

Matrix Photochemistry of Diethynyl Sulfide (3). The IR spectrum of diethynyl sulfide (**3**) in an Ar or N_2 matrix at 10 K comprises six distinctive bands, some of which exhibit splitting, possibly related to occupation of different matrix sites (Figure S1 and Table 1). Of the six bands, three bands at 2060 (2062), 705 (703), and 471 (471) cm^{-1} in N_2 (Ar) appear to exhibit little dependence on the matrix material and are associated with heavy atomic vibrational modes, whereas the other bands vary sensibly to the change of matrix material and are associated with acetylenic (≡C−H) vibrational modes.

(21) John, J. A.; Tour, J. M. *J. Am. Chem. Soc.* **1994**, *116*, 5011−5012.
(22) Chen, X.; Tolbert, L. M.; Hess, D. W.; Henderson, C. *Macromolecules* **2001**, *34*, 4104−4108.
(23) Perera, K. P. U.; Krawiec, M.; Smith, D. W., Jr. *Tetrahedron* **2002**, *58*, 10197−10203.
(24) Johnson, J. P.; Bringley, D. A.; Wilson, E. E.; Lewis, K. D.; Beck, L. W.; Matzger, A. J. *J. Am. Chem. Soc.* **2003**, *125*, 14708−14709.
(25) Rule, J. D.; Wilson, S. R.; Moore, J. S. *J. Am. Chem. Soc.* **2003**, *125*, 12992−12993.
(26) Rule, J. D.; Moore, J. S. *Macromolecules* **2005**, *38*, 7266−7273.
(27) Kawatkar, S. P.; Schreiner, P. R. *Org. Lett.* **2002**, *4*, 3643−3646.
(28) Matzger, A. J.; Lewis, K. D.; Nathan, C. E.; Peebles, S. A.; Peebles, R. A.; Kuczkowski, R. L.; Stanton, J. F.; Oh, J. J. *J. Phys. Chem. A* **2002**, *106*, 12110−12116.
(29) Lewis, K. D.; Wenzler, D. L.; Matzger, A. J. *Org. Lett.* **2003**, *5*, 2195−2197.
(30) Kim, Y. S.; McMahon, R. J. *J. Org. Chem.* **2005**, *70*, 8171−8179.
(31) Lewis, K. D.; Rowe, M. P.; Matzger, A. J. *Tetrahedron* **2004**, *60*, 7191−7196.
(32) Teles, J. H.; Hess, B. A., Jr.; Schaad, L. J. *Chem. Ber.* **1992**, *125*, 423−431.

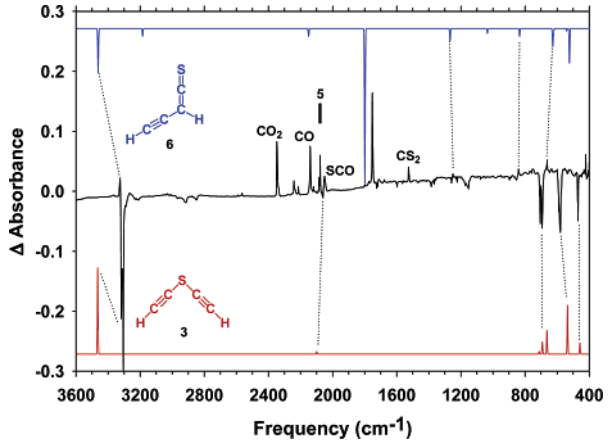

FIGURE 2. Top trace: Computed IR spectrum of ethynylthioketene (**6**) at the level of CCSD(T)/cc-pVDZ. Middle trace: IR subtraction spectrum displaying the principal growth of **6**, as well as butatrienethione (**5**), at the expense of **3**, taken 1.2 h after irradiation ($\lambda = 254$ nm; N_2, 10 K) of **3**. Bottom trace: Computed IR spectrum of diethynyl sulfide (**3**) at the level of CCSD(T)/cc-pVDZ.

Irradiation ($\lambda = 254$ nm) of matrix-isolated sulfide **3** achieves a photostationary state within 1.2 h, equivalent to 23% conversion efficiency (Figure 2). This process also brings a pale yellow color to the initially colorless sample window. Among several new species that appear during the photolysis, the major species appears to be ethynylthioketene (**6**), assigned by comparison with the computed spectrum. Other minor species are assigned to butatrienethione (**5**), as well as the small molecules CO_2, CO, SCO, C_3OS (2241 cm^{-1}),[33,34] and CS_2. At this stage, prolonged UV irradiation resulted in gradual degradation of the N_2 matrix.

The assignments of **5** and **6** were made possible through the photolysis of the anhydride described later, where IR spectra of these isomers are unambiguously measured. Specifically, the IR bands appearing at 3326, 2118, 1753, 1250, 841, and 664 cm^{-1} in Figure 2 are in accord with those of thioketene **6** obtained from the anhydride precursor. The assignment of a band at 2077 cm^{-1} (along with minor bands at 2085 and 2090 cm^{-1}) to the cumulenic stretching vibration of butatrienethione (**5**) is somewhat uncertain. When **5** is independently produced from the anhydride, bands appear at 2073, 2086, and 2090 cm^{-1} (in Ar). By contrast with the spectrum obtained upon photolysis of sulfide **3** in N_2, the feature at 2090 cm^{-1} has the greatest intensity. Shifts in frequency or intensity, such as those observed here, are often related to matrix site effects (Ar vs N_2) and/or local site effects imposed by the nature of the chemical precursor. Attempts to obtain spectra of diethynyl sulfide (**3**) and butatrienethione (**5**) in an Ar matrix were unsuccessful because of the difficulties in reproducibly generating a pure sample of **3**.[35]

Matrix Photochemistry of 2,5-Diiodothiophene (10). Photolysis ($\lambda = 254$ nm) of 2,5-diiodothiophene (**10**) affords the decay of the thiophene by ca. 7% and concurrently the generation of bands attributable to thioketene **6** (3315 and 1750 cm^{-1}) and to cumulene **5** (2084 and 2079 cm^{-1}) (Figure 3).

We anticipated the possibility that diethynyl sulfide (**3**) might be formed in the course of irradiation via a retro-Bergman cyclization process of thiophene-2,5-diyl (**4**). In fact, the spectrum revealed no evidence for the formation of the monoradical, 5-iodothiophene-2-yl, the diradical, thiophene-2,5-diyl (**4**), or the ring-opened product, diethynyl sulfide (**3**). Even if **3** were to be formed during the photolysis, it is known to rearrange to ethynylthioketene (**6**) under the irradiation conditions (Scheme 2). Photolysis of 2,5-diiodothiophene (**10**) in an Ar matrix did not exhibit appreciable photochemistry, presumably because of rapid recombination of caged radical pairs in the Ar matrix, as in the case of the photolysis of 1,4-diiodobenzene.[15,36]

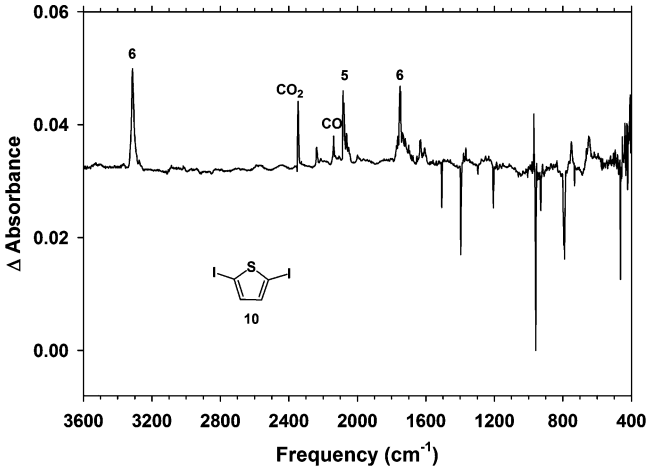

FIGURE 3. IR subtraction spectrum (N_2, 10 K) taken after irradiation ($\lambda = 254$ nm, 7% conversion) of 2,5-diiodothiophene (**10**). Ethynylthioketene (**6**) arises as the major photoproduct, along with a small amount of butatrienethione (**5**).

SCHEME 2

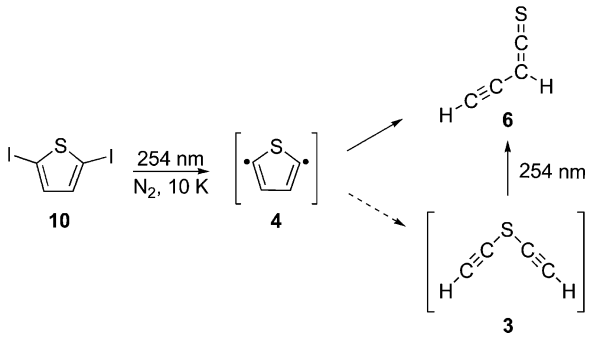

SCHEME 3

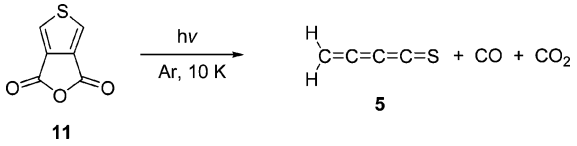

Matrix Photochemistry of Butatrienethione (5) Monitored with IR Spectroscopy. Teles et al. reported that photolysis ($\lambda = 254$ nm) of matrix-isolated 3,4-thiophenedicarboxylic acid anhydride (**11**) produces butatrienethione (**5**) as a single photoproduct (Scheme 3).[32] Indeed, our experiments ($\lambda = 254$ nm, 15.5 h, 85% conversion of anhydride) display the intense band at 2090 cm^{-1} of butatrienethione (**5**), along with CO_2 and

(33) Maier, G.; Reisenauer, H. P.; Schrot, J.; Janoschek, R. *Angew. Chem., Int. Ed. Engl.* **1990**, *29*, 1464−1466.
(34) Maier, G.; Reisenauer, H. P.; Ruppel, R. *Eur. J. Org. Chem.* **2004**, 4197−4202.
(35) Nonetheless, the experiment involving the argon matrix helps resolve the matrix site splitting. See Supporting Information for details.
(36) Wenk, H. H.; Balster, A.; Sander, W.; Hrovat, D. A.; Borden, W. T. *Angew. Chem., Int. Ed.* **2001**, *40*, 2295−2298.

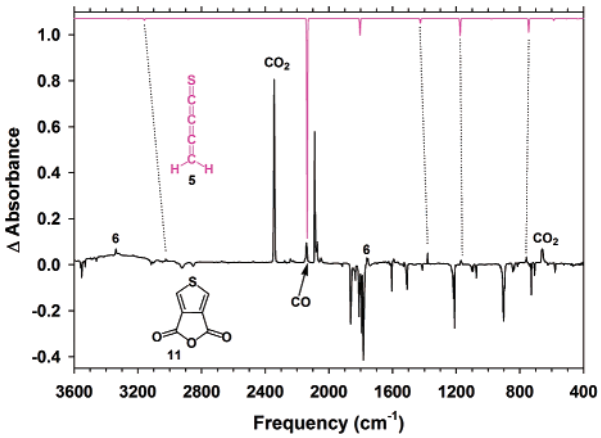

FIGURE 4. Top trace: Computed IR spectrum of butatrienethione (**5**) at the level of CCSD(T)/cc-pVDZ. Bottom trace: IR subtraction spectrum after irradiation ($\lambda = 254$ nm; Ar, 10 K; 85% photoconversion) of 3,4-thiophenedicarboxylic acid anhydride (**11**). Note two bands ascribed to a small amount of ethynylthioketene (**6**).

TABLE 2. Computed and Experimental Mid-IR Frequencies and Intensities of Butatrienethione (5)

	CCSD(T)/cc-pVDZ[a]		in Ar (this work[b])		in Ar (ref 32)	
symmetry	frequency	*I*	frequency	area	frequency	*I*
a_1	3158.9	6.1	3026	0.04	3018	(2%)
			3019			
			3015			
a_1	2136.4	942.3	2090	2.28	2089	(100%)
			2074			
a_1	1804.5	70.4	1784	0.16[c]	1783	(8%)
			1773			
a_1	1425.6	18.9	1380	0.12	1380	(6%)
a_1	1175.4	72.8	1171	0.18	1170	(8%)
b_1	744.9	58.3	759	0.13	759	(5%)
a_1	587.3	7.0				

[a] Unscaled frequencies in cm^{-1} and computed intensities in km/mol. [b] At 10 K; total integrated area under each absorption or group of closely spaced absorptions. [c] Poorly resolved due to overlap with bands of the anhydride remaining in the matrix.

CO (Figure 4). Traces of C_3OS (2242 cm^{-1}), SCO (2050 cm^{-1}), and ethynylthioketene (**6**) can also be found in the subtraction spectrum. A control experiment reveals that the anhydride can be completely destroyed using a greater irradiation intensity (less-modulated lamp output, $\lambda = 254$ nm), although the prolonged irradiation also results in the slow degradation of **5**, as judged by the loss of intensity of the band at 2090 cm^{-1}. The IR bands of butatrienethione (**5**) were assigned by comparison to the experimental spectrum (in Ar), described by Teles et al.,[32] and the computed IR spectrum (Table 2).

We are also aware that a related group of hetero-cumulenes exhibit cumulenic stretching vibrations at ca. 2100 cm^{-1} in an Ar matrix: C_5S_2 (2105 cm^{-1}),[37] C_3S_2 (2078 cm^{-1}),[37] or C_3S (2046 cm^{-1}).[38] None of these cumulenes, however, appear to interfere with our current experiments (Figure 4). Interestingly, further irradiation ($\lambda > 300$ nm) of the matrix causes the IR bands of butatrienethione (**5**) to decrease by ca. 73% and those assigned to ethynylthioketene (**6**) to emerge and grow. The conversion of **5** to **6** can be reversed with irradiation at $\lambda = 260 \pm 10$ nm, as described in the following section.

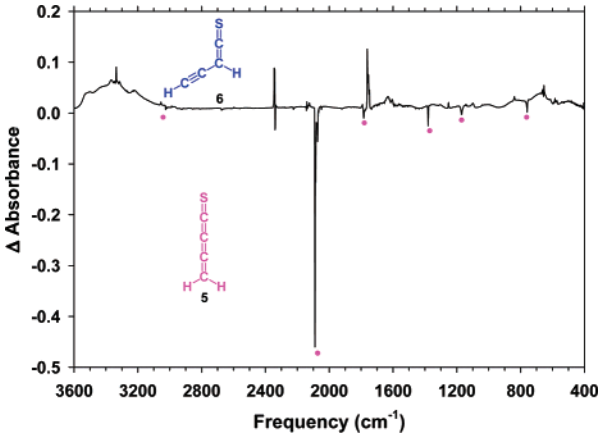

FIGURE 5. IR subtraction spectrum showing the conversion of butatrienethione (**5**) to ethynylthioketene (**6**) upon extended irradiation ($\lambda = 330 \pm 10$ nm, $373 > \lambda > 300$ nm, $\lambda > 300$ nm) of the matrix shown in Figure 4.

TABLE 3. Computed and Experimental Mid-IR Frequencies and Intensities of Ethynylthioketene (6)

	CCSD(T)/cc-pVDZ[a]		in Ar[b]	
symmetry	frequency	*I*	frequency	area
a′	3462.0	77.1	3336	0.32
			3317	
a′	3184.5	13.4	3056	0.028
a′	2149.6	13.8	2125	0.023
a′	1799	273.4	1762	1.05
			1758	
			1752	
a′	1267.8	21.2	1252	0.051
a′	1035.3	8.4	1040	0.0067
a′	834.3	13.6	840	0.065
a′	627.5	30.7	654	0.16
a″	622.7	7.9		
a″	523.4	60.5	585[c]	0.23

[a] Unscaled frequencies in cm^{-1} and computed intensities in km/mol. [b] At 10 K; total integrated area under each absorption or group of closely spaced absorptions. [c] Only major matrix site reported.

Monochromatic irradiation ($\lambda = 330 \pm 10$ nm) of the matrix containing **5** reveals small, but detectable, changes, as evidenced by the decrease of the band at 2090 cm^{-1} and the appearance of a new band at 1750 cm^{-1}. This process becomes significant upon subsequent irradiation with $373 > \lambda > 300$ nm. The new species, which grows at the expense of **5**, is assigned as ethynylthioketene (**6**), arising by an apparent [1,3]-hydrogen shift. Upon continued irradiation with $\lambda > 300$ nm, the matrix reaches a photostationary state (Figure 5). A control IR experiment reveals that, beginning with $\lambda > 300$ nm, the concentration of butatrienethione (**5**) is high (ca. 73%), which enables the IR band assignments of ethynylthioketene (**6**) to be made (Table 3).

Having established a photostationary state with $\lambda > 300$ nm, we envisaged the possibility that thioketene **6** might be converted back to butatrienethione (**5**) at a different wavelength—as in the analogous case involving the C_3H_2 isomers propadienylidene $H_2C{=}C{=}C{:}$ and propynylidene $H{-}C{-}C{-}C{-}H$.[39,40] Indeed, monochromatic irradiation at $\lambda = 260 \pm 10$ nm causes the

(37) Maier, G.; Schrot, J.; Reisenauer, H. P.; Janoschek, R. *Chem. Ber.* **1990**, *123*, 1753−1756.
(38) Maier, G.; Schrot, J.; Reisenauer, H. P.; Janoschek, R. *Chem. Ber.* **1991**, *124*, 2617−2622.
(39) Maier, G.; Reisenauer, H. P.; Schwab, W.; Cársky, P.; Hess, B. A.; Schaad, L. J. *J. Am. Chem. Soc.* **1987**, *109*, 5183−5188.
(40) Seburg, R. A.; Patterson, E. V.; Stanton, J. F.; McMahon, R. J. *J. Am. Chem. Soc.* **1997**, *119*, 5847−5856.

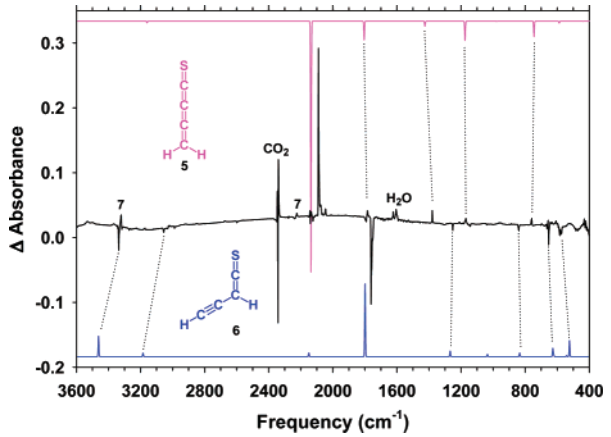

FIGURE 6. Top trace: Computed IR spectrum of **5** at the level of CCSD(T)/cc-pVDZ. Middle trace: IR subtraction spectrum displaying complete photorearrangement to **5** (10 K, Ar), upon irradiation ($\lambda = 260 \pm 10$ nm) of the matrix containing **6** that has been annealed to 35 K. Bottom trace: Computed IR spectrum of **6** at the level of CCSD(T)/cc-pVDZ. Note that two IR bands of thiol **7** are recognized.

SCHEME 4

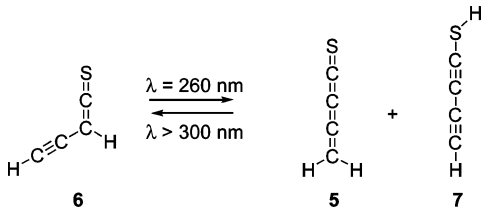

thioketene **6** to disappear completely, with concomitant growth of butatrienethione (**5**). The photoequilibration of **5** and **6** is repeatable through several cycles. (Annealing the matrix to 35 K helped resolve some of the matrix site-related bands (Figure 6).) In addition to generating the IR bands assigned to **5**, irradiation at $\lambda = 260 \pm 10$ nm always generates a peak at 3320 cm^{-1}, which subsequently disappears along with **5** upon $\lambda > 300$ nm (Figure 6). Eventually, we were able to assign the band at 3320 cm^{-1} to the acetylenic stretch of butadiynylthiol (**7**), which arises at an early stage of the irradiation of thioketene **6** at $\lambda = 260 \pm 10$ nm (Scheme 4). In fact, close examination of the spectra during the early stages of the irradiation reveals four IR bands that are plausibly attributable to butadiynylthiol (**7**): 3320, 2225, 645, and 608 cm^{-1} (Figure 7).

Matrix Photochemistry of Butatrienethione (5) Monitored with UV/Vis Spectroscopy. Analogous to the IR experiment, irradiation ($\lambda = 254$ nm; 100% conversion) of the anhydride isolated in a "thin" matrix enables the observation of a set of new electronic absorption bands (Figure 8). The new absorptions consist of two broad UV bands, λ_{max} at 219 and 255 nm, and two weak bands displaying vibrational progressions, λ_{max} at 330 and 505 nm. The two UV bands (219 and 255 nm) are ascribed to **5**, which arises as the only photoproduct observed in the IR experiment. The assignment of the two vibronic bands, however, remains problematic. The vibronic feature of the 330 nm band, which appears to be a simple Franck−Condon mode with an upper frequency of 560 cm^{-1} (mean value), cannot be assigned to either **5** or **6** because these spectral features do not change under conditions that are known to cause the photoequilibration of **5** and **6** ($\lambda > 300$ nm; Figure 9). Traces of C_3OS or its homologous species, however, might exhibit vibronic absorptions in the vicinity of 330 nm,[37,38] which are apparently silent in our current IR experiments.

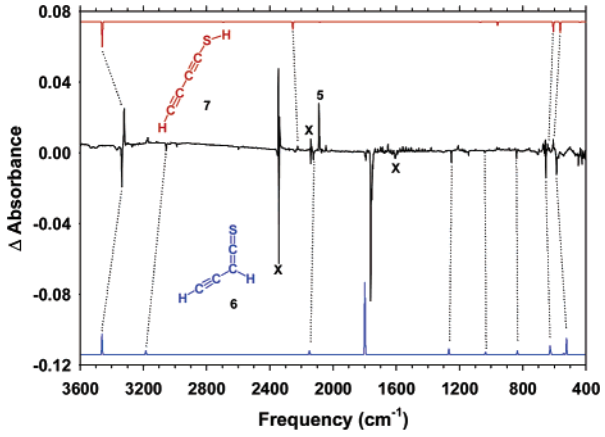

FIGURE 7. Top trace: Computed IR spectrum of butadiynylthiol (**7**) at the level of CCSD(T)/cc-pVDZ. Middle trace: IR subtraction spectrum displaying fast appearance of **7** at an early stage of the irradiation ($\lambda = 260 \pm 10$ nm; Ar, 10 K), where IR bands of **5** start to grow. Bottom trace: Computed IR spectrum of ethynylthioketene (**6**) at the level of CCSD(T)/cc-pVDZ.

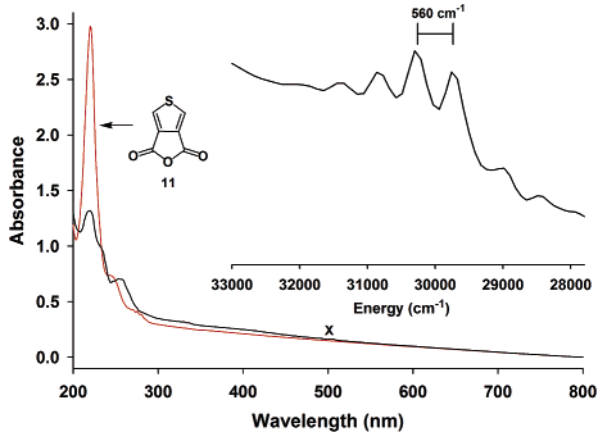

FIGURE 8. UV/vis spectra (Ar, 10 K). Red: 3,4-thiophenedicarboxylic acid anhydride (**11**) prior to irradiation. Black: butatrienethione (**5**) obtained upon irradiation ($\lambda = 254$ nm, 50 min) of the anhydride. Inset: expansion spectrum (in cm^{-1}), obtained from a separate experiment, displays the vibronic band at 330 nm. The vibronic band at 330 nm and the weak absorption at 505 nm (×) remain unassigned.

Upon irradiation ($\lambda > 300$ nm) of the matrix containing **5**, the absorptions at 219 and 330 nm decay and a broad absorption at 255 nm, which apparently overlaps the absorption assigned to **5**, appears and increases in intensity until the matrix reaches a photostationary state (Figure 9). We attribute the stronger absorption feature at 255 nm to ethynylthioketene (**6**). (The absorption at 505 nm also decreases.) If the inset spectrum in Figure 9 is closely examined, one notices that the vibronic feature at 330 nm is unchanged, although the broad absorption underneath changes during the course of the irradiation.[41] Subsequent monochromatic irradiation ($\lambda = 260 \pm 10$ nm) of the photostationary mixture allows the absorptions of **5** to recover their initial intensity and the absorption feature of **6** to disappear (Figure 9). The involvement of butadiynylthiol (**7**) in the matrix is unrecognizable in the spectrum. It is noteworthy that the visible band at 505 nm is not recovered during the irradiation at $\lambda = 260 \pm 10$ nm, thereby establishing that this spectroscopic feature is not associated with butatrienethione (**5**).

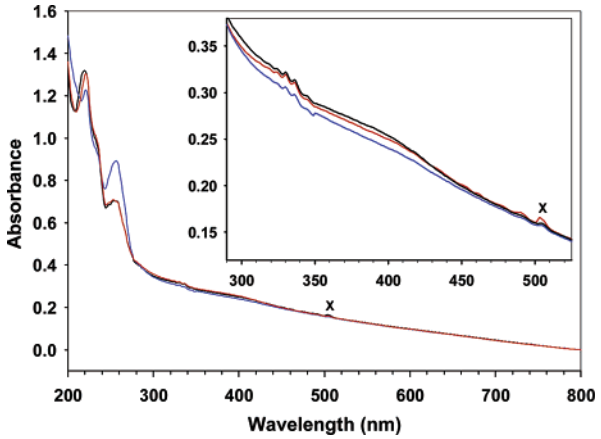

FIGURE 9. UV/vis spectra displaying reversible photoisomerization of **5** and **6**. Black: butatrienethione (**5**) (generated from 3,4-thiophenedicarboxylic acid anhydride). Blue: thioketene **6** formed upon irradiation of **5** (λ > 300 nm, 41 h; ca. 73% conversion). Red: regeneration of butatrienethione (**5**) upon irradiation of thioketene **6** ($\lambda = 260 \pm 10$ nm, 69 h). The vibronic band at 330 nm and the weak absorption at 505 nm (×) remain unassigned.

SCHEME 5[a]

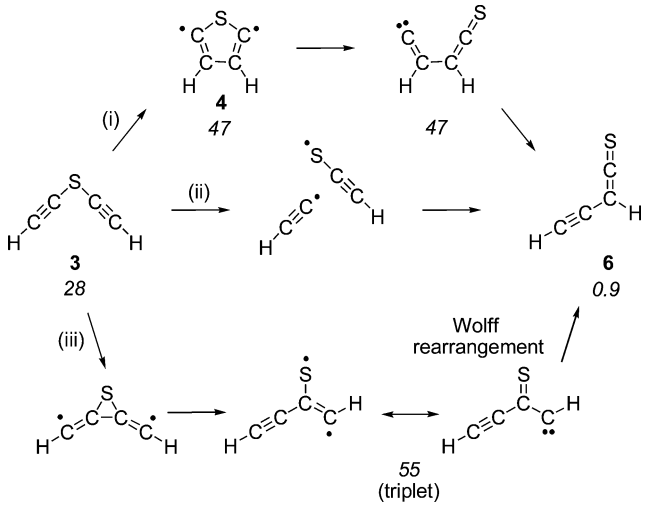

[a] Relative energy (kcal/mol) in italics.

Mechanistic Insights

Photorearrangement of Matrix-Isolated Diethynyl Sulfide (3) to Ethynylthioketene (6). At least three alternative, or competing, pathways may be envisioned for the photorearrangement of diethynyl sulfide (**3**) to thioketene **6** (Scheme 5). Each bears ample precedent, and we are unable to distinguish among them on the basis of the available evidence. Pathway (i) involves photochemical cycloaromatization to form thiophene-2,5-diyl (**4**) as a key intermediate, followed by ring opening (via C−S bond cleavage) and rearrangement to thioketene **6**. It must be noted that the potential energy diagram depicted in the scheme is the ground-state energy surface, which may or may not bear relevance to the mechanism for the photochemical process. Pathway (ii) involves photochemical cleavage of a weak C−S bond in diethynyl sulfide (**3**), with subsequent recombination of radical pairs in the matrix cage to form thioketene **6** via a net [1,3]-ethynyl shift. This pathway has been invoked in rationalizing the solution photochemistry of substituted diethynyl sulfide derivatives.[29] Pathway (iii) involves a thia-di-π-methane rearrangement,[42] with sequential formation of a three-membered thiirane,[43] a thiocarbonyl carbene, and ethynylthioketene (**6**).

SCHEME 6[a]

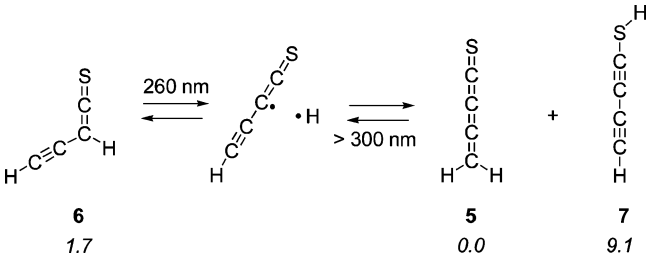

[a] CCSD(T)/cc-pVTZ energy (kcal/mol) in italics.

Photoequilibration of Butatrienethione (5), Ethynylthioketene (6), and Butadiynylthiol (7). As illustrated in Scheme 6, the three lowest-lying isomers on the C_4H_2S PES appear to photoequilibrate via [1,3]-hydrogen shifts or C−H bond homolysis followed by radical recombination in the matrix cage.

Summary

Matrix-isolated diethynyl sulfide (**3**) undergoes photochemical rearrangement to ethynylthioketene (**6**), a low-energy isomer on the C_4H_2S potential energy surface (Scheme 1). The latter is also formed from the photolysis of 2,5-diiodothiophene (**10**), indicative of the possible involvement of transient 2,5-didehydrothiophene (**4**) that rearranges either directly, or via the intermediate **3**, to thioketene **6** (Scheme 2). The three lowest-lying C_4H_2S isomers, butatrienethione (**5**), ethynylthioketene (**6**), and butadiynylthiol (**7**), appear to photoequilibrate via [1,3]-hydrogen shifts.

Methods

Computational Methods. As reported previously,[30] coupled-cluster methods implemented in a local version of ACESII program system[44] were employed to calculate geometry-optimized structures and harmonic vibrational frequencies of ground-state C_4H_2S isomers. In the current study, the CIS method in Gaussian 98[45] was employed for evaluating electronic excited states of butatrienethione (**5**). The electronic structure of diethynyl sulfide (**3**) was analyzed by Natural Resonance Theory (NRT) in NBO 5.0.[46]

Matrix-Isolation Spectroscopy. The matrix-isolation apparatus and techniques are described in the Supporting Information.

Bis(trimethylsilylethynyl) Sulfide. General procedures[47] were followed with the modification of the relative ratio of reagents, placing *n*-BuLi as the limiting reagent. This modification allows suppression of the inevitable side product, *n*-butyl trimethylsilyl-

(41) According to the CIS calculation (Supporting Information) performed at the equilibrium geometry of butatrienethione (**5**), it appears that the broad absorption at 330 nm may correlate to a weakly dipole-allowed $B\ ^1A_1 \leftarrow X\ ^1A_1$ transition, i.e., a combination of in-plane and out-of-plane $\pi \rightarrow \pi^*$ transitions of **5**. Currently, it is uncertain how the observed photochemistry has any relevance to this electronic transition of **5** and/or to the incomplete photoconversion of **5** to **6**. (As judged by the IR experiments, the photostationary mixture includes approximately 25% of the initial amount of **5**.)

(42) Hixson, S. S.; Mariano, P. S.; Zimmerman, H. E. *Chem. Rev.* **1973**, *73*, 531−551.

(43) According to an Natural Resonance Theory (NRT) analysis, the thiirane structure is recognized as a minor resonance contributor of diethynyl sulfide (**3**). See Supporting Information for details.

(44) Stanton, J. F.; Gauss, J.; Watts, J. D.; Lauderdale, W. J.; Bartlett, R. J. *Int. J. Quantum Chem.* **1992**, *S26*, 879−894.

(TMS)−ethynyl sulfide, and better control of the volatile SCl_2 during the addition.

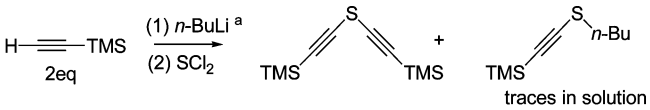

[a] Limiting reagent.

The revised procedures are as follows: To a flame-dried 100 mL round-bottom flask containing a bulky stirring bar were added 8 mL of THF (dried over Na/benzophenone) and an excess of TMS−acetylene (4 mL, 29 mmol plus the extra volume of the needle). The solution was cooled to −41 °C, then 12.2 mL (28 mmol) of *n*-BuLi (2.3 M) was added dropwise and stirred for 1 h. Meanwhile, an excess of SCl_2 (>0.9 mL, 14 mmol) was freshly distilled from stock bottle (tech. 80%) and subsequently admixed with 2 mL of THF. Then, the SCl_2/THF mixture was kept at −30 °C and syringe-transferred dropwise to the mother solution flask cooled at dry ice/acetone bath, at such rate that temperature inside the flask did not exceed −60 °C during the entire addition period. Twenty minutes after the addition, the brownish solution was allowed to warm to room temperature and quenched with 40 mL of deionized water. The ether extraction yielded 200 mL of reddish ethereal solution, which was then dried over $MgSO_4$ and gravity-filtered. Analysis of the organic layer after workup was performed via TLC with $KMnO_4$ staining, as well as GC−MS to ensure the purity of product. Solvent was removed by rotary evaporation, and the crude product was then subjected to fractional vacuum distillation; after a few drops of forerun, clear liquid was distilled at 50−56 °C (distillation head), 0.5 mmHg. ^{1}H NMR (300 MHz, $CDCl_3$): δ 0.21 (s, 18H). ^{13}C NMR (75 MHz, $CDCl_3$): δ 104.1, 86.0, −0.2. MS (EI) *m*/*z* (relative intensity): 226 (M^+, 46), 211 (100), 121 (82), 98 (34), 97 (37), 73 (80). UV/vis (λ_{max}, CH_3CN): 219 nm (ϵ = 3600 M^{-1} cm^{-1}), 229 nm (ϵ = 5910 M^{-1} cm^{-1}), 239 nm (ϵ = 6450 M^{-1} cm^{-1}).

Diethynyl Sulfide (3). It cost several experimental failures to develop an optimal procedure for the preparation of **3** and the deposition of a sample suitable for IR matrix-isolation spectroscopy. To a 25 mL round-bottom flask were added 5 mL of ethylene glycol and ca. 0.5 mL of bis(trimethylsilylethynyl) sulfide. To the well-stirred solution was added dropwise 2 equiv of $Bu_4NF{\cdot}3H_2O$ dissolved in 2 mL of ethylene glycol. The reaction mixture was stirred 20 min, prior to vacuum distillation (0.5 mmHg) of volatile substances into the first trap cooled at −78 °C for an hour. Typically, a white coating forms inside the trapping flask during this step. Then, the first trap was warmed to −41 °C and simultaneously vacuum-distilled into the deposition apparatus cooled at −180 °C for another hour. Afterward, the deposition tube was warmed to −78 °C and left under vacuum for another hour. Finally, $CDCl_3$ was added through the side arm of the deposition tube for the product analysis. ^{1}H NMR (300 MHz, $CDCl_3$): δ 3.01 (s, 2H),[48] as well as residual peaks at δ 0−2, possibly due to *n*-butyl ethynyl sulfide or mono-deprotected TMS−ethynyl ethynyl sulfide. ^{13}C NMR (75 MHz, $CDCl_3$): δ 85.1, 66.8, as well as traces of peaks at δ 82.0, 77.4, 35.0, 31.4, 21.6, 13.7, possibly due to the side products. Note in the NMR spectrum the presence of discernible side products, unavoidably produced during cycles of bulb-to-bulb distillation. Samples of **3** in a deposition tube were exposed to vacuum via several freeze−pump−thaw cycles and then co-deposited with N_2 gas for 45 min onto CsI cold window (21 K), while the deposition tube was kept in dry ice/acetone bath (−78 °C). Then, the matrix was slowly cooled to 10 K.

Preparation of 3,4-Thiophenedicarboxylic Acid Anhydride (11). As described in the literature,[49] ca. 0.55 g of 3,4-thiophenedicarboxylic acid (97%) was mixed with 8 mL of freshly distilled acetic anhydride (distilled from P_2O_5), and the solution mixture was vigorously refluxed for 2 h. After cooling, excess acetic anhydride was removed by vacuum distillation, leaving yellowish−brown solids in the flask. Subsequently, the solids were transferred to a 10 mL Erlenmeyer flask and recrystallized with a benzene and hexane mixture. Upon cooling, white needles precipitated out of solution, which were collected by vacuum filtration and rinsed with cold benzene. Light brown needles (300 mg, 61.6%) were obtained. Then, the crude anhydride was placed in a sublimation chamber and sublimed 3 h at 80−90 °C (oil bath) and 0.07 mmHg onto a water-cooled cold finger. Subsequently, white crystals (240 mg) were scraped off from the cold finger. ^{1}H NMR (300 MHz, $CDCl_3$): δ 8.10 (s, 2H).[50] ^{13}C NMR (75 MHz, $CDCl_3$): δ 156.5, 135.5, 129.5.[50] MS (EI) *m*/*z* (relative intensity): 154 (M^+, 47%), 110 (100%), 82 (47%).[50] UV/vis (λ_{max}, CH_3CN): 225 nm (ϵ = 38350 M^{-1} cm^{-1}), 250 nm (ϵ = 5020 M^{-1} cm^{-1}), and a broad shoulder around 280 nm. Given such low vapor pressure of the anhydride (mp 144−146 °C),[49] a special apparatus was designed to deposit the matrix sample (see Supporting Information).

2,5-Diiodothiophene (10) is commercially available. The sample was sublimed at room temperature and co-deposited with N_2 to form a matrix.

Acknowledgment. We gratefully acknowledge the financial support of the National Science Foundation. H.I. thanks Prof. S. Oishi (Kitasato University) for support. We thank Prof. Adam Matzger (University of Michigan), Sugumar Venkataramani (Ruhr-Universität Bochum), and Prof. Wolfram Sander (Ruhr-Universität Bochum) for stimulating discussions.

Supporting Information Available: Details concerning experimental matrix-isolation techniques; natural resonance theory analysis of diethynyl sulfide (**3**); computed electronic transitions of butatrienethione (**5**); matrix IR spectra for photolysis of diethynyl sulfide (**3**). This material is available free of charge via the Internet at http://pubs.acs.org.

JO061678L

(45) Frisch, M. J.; Trucks, G. W.; Schlegel, H. B.; Scuseria, G. E.; Robb, M. A.; Cheeseman, J. R.; Zakrzewski, V. G.; Montgomery, J. A., Jr.; Stratmann, R. E.; Burant, J. C.; Dapprich, S.; Millam, J. M.; Daniels, A. D.; Kudin, K. N.; Strain, M. C.; Farkas, O.; Tomasi, J.; Barone, V.; Cossi, M.; Cammi, R.; Mennucci, B.; Pomelli, C.; Adamo, C.; Clifford, S.; Ochterski, J.; Petersson, G. A.; Ayala, P. Y.; Cui, Q.; Morokuma, K.; Malick, D. K.; Rabuck, A. D.; Raghavachari, K.; Foresman, J. B.; Cioslowski, J.; Ortiz, J. V.; Stefanov, B. B.; Liu, G.; Liashenko, A.; Piskorz, P.; Komaromi, I.; Gomperts, R.; Martin, R. L.; Fox, D. J.; Keith, T.; Al-Laham, M. A.; Peng, C. Y.; Nanayakkara, A.; Gonzalez, C.; Challacombe, M.; Gill, P. M. W.; Johnson, B. G.; Chen, W.; Wong, M. W.; Andres, J. L.; Head-Gordon, M.; Replogle, E. S.; Pople, J. A. *Gaussian 98*, revision A.6; Gaussian, Inc.: Pittsburgh, PA, 1998.

(46) Glendening, E. D.; Badenhoop, J. K.; Reed, A. E.; Carpenter, J. E.; Bohmann, J. A.; Morales, C. M.; Weinhold, F. *NBO 5.0*; Theoretical Chemistry Institute, University of Wisconsin: Madison, WI, 2001.

(47) Verboom, W.; Schoufs, M.; Meijer, J.; Verkruijsse, H.; Brandsma, L. *Recl. Trav. Chim. Pays-Bas* **1978**, *97*, 244−246.

(48) Ashe, A. J., III; Kampf, J. W.; Waas, J. R. *Organometallics* **1995**, *14*, 3141−3142.

(49) Reinecke, M. G.; Newsom, J. G.; Chen, L.-J. *J. Am. Chem. Soc.* **1981**, *103*, 2760−2769.

(50) Nielsen, C. B.; Bjørnholm, T. *Org. Lett.* **2004**, *6*, 3381−3384.